

A&A manuscript no.
(will be inserted by hand later)

Your thesaurus codes are:
06 (08.22.1; 08.15.1; 08.04.1)

Theoretical models for classical Cepheids: V. Multiwavelength relations

F. Caputo¹, M. Marconi², I. Musella²

¹ Osservatorio Astronomico di Roma, Via di Frascati 33, I-00040 Monteporzio Catone, Italy

² Osservatorio Astronomico di Capodimonte, Via Moiariello 16, I-80131 Napoli, Italy
email: caputo@coma.mporzio.astro.it, marcella@na.astro.it, ilaria@na.astro.it

Received; accepted

Abstract. From a theoretical study based on nonlinear, nonlocal and time-dependent convective pulsating models at varying mass and chemical composition, we present the predicted Period-Luminosity, Period-Color, Color-Color and Period-Luminosity-Color relations in the *BVRIJK* bands for Classical Cepheids. All the theoretical relations are, in various degrees, metallicity dependent and the comparison with observed data for MC and Galactic Cepheids show a fair agreement which supports the validity of the pulsating models.

Key words: Stars: variables: Cepheids – Stars: oscillations – Stars: distances

1. Introduction

Since the Leavitt (1912) discovery of the relationship between period and apparent magnitude for Cepheids in the Magellanic Clouds, these variables have been playing a fundamental role in the determination of distances to Local Group galaxies, in the calibration of various secondary distance indicators and finally in the evaluation of the Hubble constant H_0 . A considerable amount of observational studies have been devoted to the calibration of their characteristic Period-Luminosity (*PL*) and Period-Luminosity-Color (*PLC*) relations, e.g. via the Baade-Wesselink method (Ripepi et al. 1997; Gieren et al. 1998 and references therein), or making use of Cepheids with distances from Galactic open cluster main-sequence fitting (Turner et al. 1998 and references therein), or adopting the Large Magellanic Cloud (LMC) distance found in other independent ways (see Walker 1999).

The most important question to be answered is whether the **bolometric *PL*** and *PLC* are *universal*, as early suggested by Iben & Renzini (1984), or depending on the chemical abundances of the variables. This is a fundamental point since **if there is a metallicity effect on the relations in the various photometric bands and**

the galaxies whose distances we are deriving have metallicities different from the calibrating Cepheids, then a **significant correction could be necessary**. In recent times, the occurrence of a metallicity effect has become more and more evident, with the observational tests of this effect suggesting that metal-rich Cepheids are brighter than metal-poor Cepheids at fixed period (see Kochanek 1997; Beaulieu et al. 1997; Sasselov et al. 1997; Kennicutt et al. 1998). As for theoretical estimates, models based on linear pulsation calculations suggest a very low effect (Chiosi et al. 1993; Saio & Gautschy 1998; Alibert et al. 1999), whereas nonlinear, nonlocal and time-dependent convective pulsating models suggest that both the zero point and the slope of the predicted *PL* relations depend on metallicity, with the amplitude of the metallicity effect decreasing at the longer wavelengths (Bono et al. 1999b [Paper II]). Moreover, these models show that metal-rich Cepheids are on average intrinsically fainter than the metal-poor ones, at fixed period.

It is worth noticing that all the observational efforts rely on the assumption that the slope of the *PL* relation for different passbands is that found for LMC Cepheids, leading us to suspect that forcing the slope of the multiwavelength relations to be constant may introduce some systematic errors in the attempt of disentangling reddening from metallicity effects. On the other hand, at variance with the linear-nonadiabatic approach which supplies only the blue edge of the instability strip ¹, the models presented in Paper II provide fine constraints on both blue and red limits of the pulsation, thus avoiding dangerous *ad hoc* assumptions on the width of the instability strip (see also Tanvir 1999). These models give also the pulsation amplitude and the predicted mean magnitudes of the pulsator.

¹ Linear red edge estimates by Chiosi et al. (1993) and by Alibert et al. (1999) were fixed, more or less tentatively, at the effective temperature where the growth rate attains its maximum value. However, the nonlinear results suggest that such an assumption is far from being adequate (Bono et al. 1999c [Paper III]).

The theoretical PL and PLC relations presented in Paper II deal with the intensity-weighted $\langle M_B \rangle$, $\langle M_V \rangle$ and $\langle M_K \rangle$ magnitudes. In order to have a full insight into the metallicity effect, and considering that the HST observations of extragalactic Cepheids consider the I band, in this paper we present the full set of theoretical relations (i.e. Period-Luminosity, Period-Color, Color-Color and Period-Luminosity-Color) in the $BVRIJK$ bands. The predicted relations are reported in Sect. 2, while Sect. 3 gives brief comparisons of our theoretical results against observed data for calibrating Cepheids. Some final remarks close the paper.

2. Predicted relations

The nonlinear convective pulsating models adopted in this paper are computed with four values of the stellar mass ($M/M_\odot = 5, 7, 9, 11$) and three chemical compositions ($Y=0.25, Z=0.004$; $Y=0.25, Z=0.008$; $Y=0.28, Z=0.02$), taken as representative of Cepheids in the Magellanic Clouds and in the Galaxy. The basic assumptions on the input physics, computing procedures and the adopted mass-luminosity relation have been already discussed in Bono et al. (1998), Bono et al. (1999a [Paper I]) and Paper III and will not be repeated. **Here we wish only to remark that the whole instability strip moves toward lower effective temperatures as the metallicity increases and, as a consequence, that the bolometric magnitude of the pulsators increases as the metal abundance increases (see Fig. 2 in Paper II).**

2.1. Period-Luminosity

From the bolometric light curves of our pulsating models and adopting the grid of atmosphere models provided by Castelli et al. (1997a,b), we first derive the predicted intensity-weighted mean magnitude $\langle M_\lambda \rangle$ of pulsators for the $BVRIJK$ passbands². The fundamental pulsators plotted in Fig. 1, where the different lines depict the blue and red limits of the pulsation region at the various compositions, show that the metal abundance effects on the predicted location and width of the instability strip are significantly dependent on the photometric passband. In particular, the models confirm early results (e.g., see Laney & Stobie 1994; Tanvir 1999 and reference therein) that infrared magnitudes are needed to reduce both the intrinsic scatter and the metal abundance dependence of the PL relation.

This matter has been already discussed in Paper II on the basis of the predicted PL_V and PL_K relations derived under the assumption of a uniformly populated instability strip. However, since the PL is a “statistical” relation which provides the average of the Cepheid magnitudes $\overline{M_\lambda}$ at a given period, we decide to estimate the

² These atmosphere models do not allow the calculation of synthetic H magnitudes.

Fig. 1. Location in the $\log P - \langle M_V \rangle$ and $\log P - \langle M_K \rangle$ plane of fundamental pulsators with different chemical compositions and masses (from left to right: 5, 7, 9 and $11M_\odot$). The lines depict the predicted edges of the instability strip.

Fig. 2. Period-magnitude distribution of fundamental pulsators at varying metallicity and photometric bandpass. Dashed lines and solid lines refer to the quadratic and linear PL relations given in Table 1 and Table 2, respectively.

effect of a different pulsator population. Thus, following the procedure outlined by Kennicutt et al. (1998), for each given chemical composition we populate the instability strip³ with 1000 pulsators and a mass distribution as given by $dn/dm = m^{-3}$ over the mass range $5-11M_\odot$. The corresponding luminosities are obtained from the mass-luminosity relation derived from canonical evolutionary models, i.e. with vanishing efficiency of convective core overshooting (see Bono & Marconi 1997; Paper II; Paper III).

Fig. 2 shows the resulting $\log P - M_\lambda$ distribution of fundamental pulsators with the three selected metallicities. We derive that the pulsator distribution becomes more and more linear by going toward the infrared and that, aiming at reducing the intrinsic scatter of PL , the pulsator distributions in the $\log P - M_B$, $\log P - M_V$ and $\log P - M_R$ planes are much better represented by a quadratic relation. The dashed lines in Fig. 2 show the quadratic least square fit ($\overline{M_\lambda} = a + b \log P + c \log P^2$), while the solid lines refer to the linear approximation ($\overline{M_\lambda} = a + b \log P$). The values for the coefficients a , b and c of each PL_λ relation are listed in Table 1 (quadratic solution) and Table 2 (linear solution), together with the rms dispersion (σ) of M_λ about the fit. However, we wish to remark that the present solutions refer to a specific pulsator distribution and that different populations may modify the results. As a matter of example, if the longer periods ($\log P \geq 1.5$) are rejected in the final fit, then the predicted linear PL relations become steeper and the intrinsic dispersion in the BVR bands is reduced (see Table 3).

As a whole, each predicted PL_λ relation seems to become steeper at the lower metal abundances, with the amplitude of the effect decreasing from B to K filter. Moreover, the slope and the intrinsic dispersion of the predicted

³ The location of the instability strip is constrained by the predicted blue and red edges.

Fig. 3. Slope and intrinsic dispersion of the predicted linear PL relations with different bandpass.

PL relation at a given Z decrease as the filter wavelength increases (see Fig. 3 for the linear relations), in close agreement with the observed trend (e.g. see Fig. 6 in Madore & Freedman 1991).

In closing this section, let us observe that the adopted way to populate the instability strip allows PL relations only for the “static” magnitudes (the value the star would have were it not pulsating), while the observations deal with the mean magnitudes averaged over the pulsation cycle [$\langle m_\lambda \rangle$ if magnitude-weighted and $\langle m_\lambda \rangle$ if intensity-weighted]. It has been recently shown (Caputo et al. 1999 [Paper IV]) that the differences among static and mean magnitudes and between magnitude-weighted and intensity-weighted averages are always smaller than the intrinsic scatter of the PL relation (~ 0.1 mag for V magnitudes and ≤ 0.01 mag for K magnitudes). Here, given the marginal agreement of the coefficients in Table 1, Table 2 and Table 3 with the values given in Paper IV, we conclude that the additional effect on the intrinsic scatter of the PL relations, as due to different Cepheid populations, is negligible, provided that a statistically significant sample of variables is taken into account.

2.2. Period-Color and Color-Color

The three methods of deriving the mean color over the pulsation cycle use either $(m_j - m_i)$, the average over the color curve taken in magnitude units, or $\langle m_j - m_i \rangle$, the mean intensity over the color curve transformed into magnitude, or $\langle m_j \rangle - \langle m_i \rangle$, the difference of the mean intensities transformed into magnitude, performed separately over the two bands. In Paper IV it has been shown that there are some significant differences between static and synthetic mean colors, and that the predicted $(m_j - m_i)$ colors are generally redder than $\langle m_j \rangle - \langle m_i \rangle$ colors, with the difference depending on the shape of the light curves, in close agreement with observed colors for Galactic Cepheids. As a matter of example, the predicted difference $(B - V) - [\langle B \rangle - \langle V \rangle]$ ranges from 0.02 mag to 0.08 mag, whereas $(V - K) - [\langle V \rangle - \langle K \rangle]$ is in the range of 0.014 mag to 0.060 mag.

Fig. 4 shows the pulsator synthetic mean colors as a function of the period for the three different metallicities. Since, given the finite width of the instability strip, also the PC relation is a “statistical” relation between period and the average of the mean color indices CI , we follow the procedure of Sect. 2.1. It is evident from Fig. 4 that the pulsator distribution shows a quadratic behavior, as well as that the intrinsic dispersion of PC relations al-

Fig. 4. Location in the period-color plane of fundamental pulsators with different chemical compositions and masses. The lines depict the linear PC relations given in Table 4.

Fig. 5. The color-color plane of fundamental pulsators. The lines depict the CC relations at varying metallicities (see Table 5).

lows reddening estimates within ~ 0.07 mag, on average. However, as far as they could help, we present the predicted relations $\overline{CI} = A + B \log P$ at the various compositions. The relations are plotted in Fig. 4 and the A and B coefficients are listed in Table 4 together with the rms deviation of the color about the fit (σ). Note that also the slope of the predicted PC relations depends on the metal abundance, increasing with increasing Z .

As for the color-color (CC) relations, Fig. 5 shows that the spurious effect due to the finite width of the instability strip is almost removed. For this reason, from our pulsating models we derive a set of color-color (CC) relations correlating $\langle B \rangle - \langle V \rangle$ with $\langle V \rangle - \langle R \rangle$, $\langle V \rangle - \langle I \rangle$, $\langle V \rangle - \langle J \rangle$ and $\langle V \rangle - \langle K \rangle$, but similar relations adopting $(m_j - m_i)$ or $\langle m_j - m_i \rangle$ colors can be obtained upon request. The predicted CC linear relations are given in Table 5, while Fig. 5 shows the pulsator distribution in the color-color plane. One may notice that the intrinsic scatter of the theoretical relations is very small, with the rms dispersion of $\langle B \rangle - \langle V \rangle$ about the fit smaller than 0.01 mag.

2.3. Period-Luminosity-Color

Since the pioneering paper by Sandage (1958), Sandage & Gratton (1963) and Sandage & Tammann (1968), it is well known that if the Cepheid magnitude is given as a function of the pulsator period and color, i.e. if the Period-Luminosity-Color relation is considered, then the tight correlation among the parameters of individual Cepheids is reproduced (see also Laney & Stobie 1986; Madore & Freedman 1991; Feast 1995 and references therein).

In Paper II it has been shown that the intrinsic scatter of the PLC relations in the visual ($\langle M_V \rangle$, $\langle B \rangle - \langle V \rangle$) and infrared ($\langle M_V \rangle$, $\langle V \rangle - \langle K \rangle$) is ~ 0.04 mag. Furthermore, we showed in Paper IV that the systematic effect on the predicted visual PLC relations, as due to the adopted method of averaging magnitudes and colors over the pulsation cycle, are always larger than the intrinsic scatter of the relation. For this reason in this paper we present only the predicted PLC

Fig. 6. Projection onto a plane of the predicted *PLC* relations ($\langle B \rangle - \langle V \rangle$ and $\langle V \rangle - \langle R \rangle$ colors) for fundamental pulsators with different metallicities (see Table 6).

Fig. 7. As in Fig. 6, but with $\langle V \rangle - \langle I \rangle$ and $\langle V \rangle - \langle J \rangle$ colors.

Fig. 8. As in Fig. 6, but with $\langle V \rangle - \langle K \rangle$ colors.

relations $\langle M_V \rangle = \alpha + \beta \log P + \gamma[\langle M_V \rangle - \langle M_\lambda \rangle]$, but similar relations for magnitude-weighted values can be obtained upon request.

From the least square solutions through the fundamental models we derive the coefficients α , β and γ presented in Table 6, together with the residual dispersion (σ) of $\langle M_V \rangle$ about the fit. Figs. 6-8 illustrate the remarkably small scatter of the *PLC* relations (see Fig. 1 for comparison). Moreover, one may notice that adopting $B-V$ color, the metal-rich Cepheids are brighter than metal-poor ones with the same period and color (see lower panel of Fig. 6), whereas the opposite trend holds with $V-K$ color (see Fig. 8). As a “natural” consequence, the predicted relationship with $V-I$ color (lower panel of Fig. 7) turns out to be almost independent of the metal abundance.

In order to complete the theoretical framework for classical Cepheids, we have finally considered the Wesenheit quantities W (Madore 1982) which are often used to get a reddening-free formulation of the *PL* relation. With A_λ giving the absorption in the λ -passband, one has

$$W(B, V) = V - [A_V / (A_B - A_V)](B - V)$$

$$W(B, V) = V_0 + A_V - [A_V / (A_B - A_V)][(B - V)_0 + (A_B - A_V)]$$

$$W(B, V) = V_0 - [A_V / (A_B - A_V)](B - V)_0,$$

$$W(V, R) = R - [A_R / (A_V - A_R)](V - R)$$

$$W(V, R) = R_0 + A_R - [A_R / (A_V - A_R)][(V - R)_0 + (A_V - A_R)]$$

$$W(V, R) = R_0 - [A_R / (A_V - A_R)](V - R)_0,$$

etc....

Table 7 gives the coefficients of the theoretical reddening-free *PL* [hereinafter *WPL*] relations derived from our fundamental models. Note that present results adopt

Fig. 9. Predicted *WPL* relations of fundamental pulsators with different chemical compositions (see Table 7).

Fig. 10. Predicted *WPL* relations of fundamental pulsators with different chemical compositions (see Table 7).

$A_V/E_{B-V} = 3.1$, $A_R/E_{V-R} = 5.29$, $A_I/E_{V-I} = 1.54$, $A_J/E_{V-J} = 0.39$ and $A_K/E_{V-K} = 0.13$ from the Cardelli et al. (1989) extinction model, but formulations using different ratios of total to selective absorption can be obtained upon request.

Figs. 9-10 show the theoretical Wesenheit quantities as a function of the period, together with the predicted relations. From a comparison of Table 7 with Table 2 one derives that the intrinsic scatter of $W(B, V)PL$ and $W(V, R)PL$ is significantly lower than the dispersion of *PL*, while no significant improvement occurs with $W(V, I)PL$ and somehow larger dispersions are found $W(V, J)PL$ and $W(V, K)PL$.

Moreover, the comparison between Figs. 9-10 and Figs. 6-8 discloses the deep difference between *PLC* and *WPL* relations (see also Madore & Freedman 1991). The former ones are able to define accurately the properties of individual Cepheids within the instability strip, whereas the latter ones are thought to cancel the reddening effect. As a consequence, provided that the variables are at the same distance and have the same metal abundance, the scatter in observed *PLC* relations should depend on **errors in the adopted** reddening, whereas the scatter in observed *WPL* relations is a residual effect of the finite width of the strip.

3. Comparison with Galactic Cepheids

The principal aim of this paper is to present a wide homogeneous theoretical scenario for Cepheid studies. The analysis of observed pulsational properties is out of our present intentions, but it seems necessary to verify the reliability of our models against well studied variables. For this purpose, we take into consideration the sample of calibrating Galactic Cepheids studied by Gieren et al. (1998, [GFG]) and by Laney & Stobie (1994, [LS]). To the intensity mean magnitudes *BVJK* magnitudes we add the $\langle I \rangle$ magnitudes as derived from $\langle V \rangle - \langle I \rangle - (V - I) = -0.03$ mag, where the magnitude-weighted (V-I) colors are by Caldwell & Coulson (1987). Such a constant correction, suggested by GFG, is confirmed (see Fig. 11) from our synthetic mean colors. Note that, according to GFG, we excluded SV Vul, GY Sge and S Vul for problems with

Fig. 11. Predicted difference between $\langle V \rangle - \langle I \rangle$ and $(V-I)$ colors for fundamental pulsators with different masses and chemical compositions. The solid line refers to a difference of -0.03 mag.

Fig. 12. (*lower panel*) Wesenheit quantities of fundamental pulsators in comparison with the OGLE *WPL* relation. (*upper panel*) OGLE *PLC* relation applied to fundamental pulsators.

Fig. 13. Calibrating Galactic Cepheids (dots) in comparison with predicted *PL* relations with $Z=0.02$ (dotted line). Data from Laney & Stobie (1994 [LS]).

a variable period and EV Sct, SZ Tau and QZ Nor for uncertainty with regard to the pulsation mode.

Before analyzing the calibrating Galactic Cepheids, let us briefly consider the recent results on Magellanic Clouds Cepheids provided by the OGLE II microlensing survey (Udalski et al. 1999). The final PL_V and PL_I relations given by these authors for Cepheids with $\log P \leq 1.5$, are $M_V = -1.18 - 2.765 \log P$ and $M_I = -1.66 - 2.963 \log P$, with a LMC distance modulus $\mu_{LMC} = 18.22$ mag. The data in Table 3 with $Z=0.008$ yield $M_V = -1.37 - 2.75 \log P$ and $M_I = -1.95 - 2.98 \log P$, namely a predicted slope in close agreement with OGLE measurements but a zero-point which is brighter by roughly 0.24 mag, suggesting $\mu_{LMC} = 18.46$ mag, a value which fits the recent upward revision of the LMC distance derived from field red clump stars (Zaritsky 1999).

As for the $W(V, I)PL$ relation presented by Udalski et al. (1999), we find that its slope (-3.28) is in fair agreement with the results (-3.17) of our models with $Z=0.008$ (see also the lower panel of Fig. 12). Conversely, the OGLE PLC_I relation discloses a significative difference with respect to our predicted relations. As shown in the upper panel of Fig. 12, it seems that the OGLE color-term is not able to fully remove the effect of the finite width of the instability strip (as a matter of comparison, see the lower panel of Fig. 7). At the moment we cannot explain such a disagreement and we expect the release of LMC and SMC data to test the full set of our predictions.

Passing to the Galactic Cepheids, Fig. 13 and Fig. 14 show the predicted linear *PL* relations with $Z=0.02$ (dotted line) in comparison with the calibrating Cepheids (dots) from LS and GFG, respectively. Note that both the reddening and true distance modulus given by the au-

Fig. 14. Calibrating Galactic Cepheids (dots) in comparison with predicted *PL* relations with $Z=0.02$ (dotted line). Data from Gieren et al. (1998 [GFG]).

Fig. 15. Calibrating Galactic Cepheids (dots) from Laney & Stobie (1994 [LS]) and Gieren et al. (1998 [GFG]), in comparison with OGLE *PL* relations for LMC and SMC Cepheids (dashed-dotted line).

Fig. 16. As in Fig. 13, but for predicted *PLC* relations.

Fig. 17. As in Fig. 14, but for predicted *PLC* relations.

thors are adopted. We find a fair agreement in the infrared, whereas in the V and I bands the observed Cepheids with the longer periods appear brighter than the predicted relations. This could suggest that these luminous variables have lower metallicities than the currently adopted value $Z=0.02$ (see Fry & Carney 1997) or be near the blue edge of the instability strip. One could also suspect that the predicted slopes with $Z=0.02$ are smaller than the actual ones. This seems supported by Fig. 15 where the steeper PL_V relation provided by Udalski et al. (1999) is taken into account.

However, in order to remove the effects of the finite width of the instability strip, let us apply our predicted *PLC* relations to the calibrating Cepheids. Figs. 16-17 disclose that predictions and observed data are now in a better agreement. Meanwhile, there are some evidence that the calibrating Galactic Cepheids lie on the average below the theoretical *PLC* relations with $Z=0.02$. In other words, our predicted relations yield somehow larger true distance moduli than those given by LS and GFG. Specifically, the left panels of Fig. 18 show that the difference between LS and GFG data and the results of our predicted PLC_{VI} relation with $Z=0.02$, by adopting the reddening values listed by these authors, have a significant period dependence. This trend cannot be ascribed to our color and period term since a quite similar behavior is present in the right panels which refer to the PLC_{VI} relation given by Udalski et al. (1999). **Notwithstanding the different values of the period and color terms, one finds a similar trend, with the OGLE relation**

Fig. 18. True distance modulus of Galactic Cepheids from the PLC_{VI} relation in comparison with Laney & Stobie (1994 [LS]) and Gieren et al. (1998 [GFG]) data. The left panel refer to the predicted relation with $Z=0.02$, while the right panels refer to the OGLE result for LMC and SMC Cepheids.

Fig. 19. Galactic Cepheids BVI reddenings from predicted CC relations with $Z=0.02$ in comparison with LS93 (circles) and LS94 (dots) values.

Fig. 20. Predicted $(B-V)-(V-I)$ relation with $Z=0.02$ (dotted line) in comparison with the intrinsic locus of Galactic Cepheids. The solid line and the dashed line refer to the labelled solutions, as given by Dean, Warren & Cousins (1978).

suggesting smaller distances than those listed by LS and GFG.

On the other hand, we show in Fig. 19 that the BVI reddenings⁴ derived from the predicted color-color relation with $Z=0.02$ are slightly lower than those given by LS and GFG. The origin of the discrepancy could be found in Fig. 20, where our predicted color-color relation with $Z=0.02$ (dotted line) is plotted together with the two quadratic relations given by Dean et al. (1978) for the intrinsic color-color locus of the Galactic Cepheids (solid line and dashed line). Since observational studies generally adopt the solution depicted with the solid line, the reason for which our predicted CC relation yields slightly smaller BVI reddenings is explained. This **could provide** the key to understand the difference in the true distance moduli.

4. Summary

From nonlinear, nonlocal and time-dependent convective pulsating models we have derived a set of homogeneous PL , PC , CC , PLC and WPL relations in the $BVRIJK$ passbands at varying chemical composition. We find that the predicted relations are, in various degrees, metallicity dependent, suggesting that the adoption of *universal* relations for Cepheid studies should be treated with caution.

The slope of the predicted relations with $Z=0.004$ - 0.008 matches the results of LMC and SMC Cepheids col-

lected during the OGLE II microlensing survey (Udalski et al. 1999), but our zero points suggest a larger LMC distance, in agreement with the suggestions by Zaritsky (1999).

As for the comparison of the predicted relations at $Z=0.02$ with the observed data of calibrating Galactic Cepheids, we find a fair agreement even though the slope of our PL_V and PL_I relations seems shallower than observed. This is the consequence of the significant metallicity dependence in the predicted relations and we believe that a careful analysis (of larger samples of Galactic Cepheids) which takes into account the actual metallicity dispersion is required to settle the question.

Special requests for other theoretical relations can be addressed to M. Marconi.

Acknowledgements. We deeply thank the referee (Dr. Bersier) for several valuable comments which improved the first version of the paper. Financial support for this work was provided by the Ministero dell'Università e della Ricerca Scientifica e Tecnologica (MURST) under the scientific project "Stellar Evolution" (Vittorio Castellani, coordinator).

References

- Alibert Y., Baraffe I., Hauschildt P., Allard, F. 1999, A&A 344, 551
- Beaulieu J. P., Krockenberger M., Sasselov D. D. et al. 1997, A&A 318, L47
- Bono G., Marconi M. 1997, MNRAS 290, 353
- Bono G., Caputo F., Marconi M. 1998, ApJ 497, L43
- Bono G., Marconi M., Stellingwerf R. F. 1999a, ApJS 122, 167 [Paper I]
- Bono G., Caputo F., Castellani V., Marconi M. 1999b, ApJ 512, 711 [Paper II]
- Bono G., Castellani V., Marconi M. 1999c, ApJ, in press [Paper III]
- Caldwell J. A. R., Coulson I. M. 1987, AJ 93, 1090
- Caputo F., Marconi M., Ripepi V. 1999, ApJ 525, 784 [Paper IV]
- Cardelli J. A., Clayton G. C., Mathis J. S. 1989, ApJ 345, 245
- Castelli F., Gratton R. G., Kurucz R. L. 1997a, A&A 318, 841
- Castelli F., Gratton R. G., Kurucz R. L. 1997b, A&A 324, 432
- Chiosi C., Wood P. R., Capitanio N. 1993, ApJS 86, 541
- Dean J. F., Warren P. R., Cousins, A. W. 1978, MNRAS 183, 569
- Feast, M. W. 1995, in IAU Colloq. 155, Astrophysical Applications of Stellar Pulsation, eds. R.S. Stobie, P.A. Whitelock (San Francisco: ASP), 209
- Fry A. M., Carney B. W. 1997, ApJ 113, 1073
- Gieren W. P., Fouqué P., Gómez M. 1998, ApJ 496, 17
- Iben I., Renzini A. 1984, Physics Reports 105, 6
- Kennicutt R. C., Stetson P. B., Saha A. et al. 1998, ApJ 498, 181
- Kochanek C. S. 1997, ApJ 491, 13
- Laney C. D., Stobie R. S. 1986, MNRAS 222, 449
- Laney C.D., Stobie R. S. 1993, MNRAS 263, 291
- Laney C. D., Stobie R. S. 1994, MNRAS 266, 441 (LS)
- Leavitt H. 1912 Harvard Circular 173 (reported by E.C. Pickering)

⁴ We adopt the ratios of total to selective absorption in the VI bands from Caldwell & Coulson (1987) and Laney & Stobie (1993).

Madore B. F. 1982, ApJ 253, 575
 Madore B. F., Freedman W. L. 1991, PASP 103, 933
 Ripepi V., Barone F., Milano L., Russo G. 1997, A&A 318, 797
 Saio H., Gautschy A. 1998, ApJ 498, 360
 Sandage A. 1958, ApJ 127, 513
 Sandage A., Gratton L. 1963, in Star Evolution, ed. L. Gratton
 (New York, Academic Press), p. 11
 Sandage A., Tammann, G. 1968, ApJ, 151, 531
 Sasselov D. D., Beaulieu J. P., Renault, C. et al. 1997, A&A
 324, 471
 Tanvir N. R. 1999, in Post-Hipparcos Cosmic Candles, eds. A.
 Heck, F. Caputo (Dordrecht, Kluwer Academic Publish-
 ers), p. 17
 Turner A., Ferrarese L., Saha A. et al. 1998, ApJ 505, 207
 Udalski A., Szymanski M., Kubiak M. et al. 1999, Acta Astro-
 nomica 49, 201
 Walker, A., 1999, in Post-Hipparcos Cosmic Candles, eds. A.
 Heck, F. Caputo (Dordrecht, Kluwer Academic Publish-
 ers), p. 125
 Zaritsky D. 1999, astro-ph/9908363, accepted for publication
 on AJ

Table 1. Theoretical PL relations for fundamental pul-
 sators. Quadratic solutions: $\overline{M}_\lambda = a + b \log P + c \log P^2$.

Z	a	b	c	σ
\overline{M}_B				
0.004	-0.01±0.06	-4.81±0.10	1.14±0.06	0.24
0.008	-0.21±0.06	-4.17±0.13	0.94±0.06	0.26
0.002	-0.93±0.04	-2.43±0.09	0.39±0.04	0.21
\overline{M}_V				
0.004	-0.69±0.04	-4.43±0.10	0.81±0.05	0.18
0.008	-0.86±0.04	-3.98±0.09	0.67±0.05	0.19
0.02	-1.41±0.03	-2.75±0.07	0.30±0.03	0.16
\overline{M}_R				
0.004	-1.08±0.04	-4.28±0.08	0.67±0.04	0.15
0.008	-1.22±0.04	-3.91±0.08	0.56±0.04	0.16
0.02	-1.69±0.03	-2.88±0.06	0.26±0.03	0.13
\overline{M}_I				
0.004	-1.48±0.03	-4.16±0.07	0.56±0.03	0.13
0.008	-1.59±0.03	-3.84±0.07	0.47±0.03	0.13
0.02	-1.98±0.02	-2.99±0.05	0.23±0.02	0.11
\overline{M}_J				
0.004	-1.97±0.02	-3.97±0.05	0.40±0.02	0.09
0.008	-2.04±0.02	-3.73±0.05	0.33±0.02	0.10
0.02	-2.32±0.01	-3.08±0.03	0.12±0.02	0.08
\overline{M}_K				
0.004	-2.42±0.01	-3.81±0.03	0.26±0.01	0.06
0.008	-2.45±0.01	-3.65±0.03	0.21±0.01	0.06
0.02	-2.63±0.01	-3.19±0.02	0.06±0.01	0.05

Table 2. Theoretical PL relations for fundamental pulsators. Linear solutions: $\overline{M}_\lambda = a + b \log P$.

Z	a	b	σ
\overline{M}_B			
0.004	-1.07±0.02	-2.49±0.02	0.27
0.008	-1.08±0.02	-2.24±0.02	0.28
0.02	-1.28±0.02	-1.64±0.02	0.22
\overline{M}_V			
0.004	-1.44±0.02	-2.79±0.02	0.20
0.008	-1.48±0.02	-2.60±0.02	0.20
0.02	-1.68±0.01	-2.15±0.01	0.16
\overline{M}_R			
0.004	-1.71±0.01	-2.90±0.01	0.17
0.008	-1.74±0.01	-2.75±0.01	0.17
0.02	-1.92±0.01	-2.36±0.01	0.14
\overline{M}_I			
0.004	-2.00±0.01	-3.00±0.01	0.14
0.008	-2.03±0.01	-2.88±0.01	0.14
0.02	-2.18±0.01	-2.53±0.01	0.12
\overline{M}_J			
0.004	-2.34±0.01	-3.15±0.01	0.10
0.008	-2.35±0.01	-3.06±0.01	0.10
0.02	-2.43±0.01	-2.84±0.01	0.08
\overline{M}_K			
0.004	-2.66±0.01	-3.29±0.01	0.07
0.008	-2.65±0.01	-3.23±0.01	0.07
0.02	-2.68±0.01	-3.08±0.01	0.05

Table 3. Theoretical PL relations for fundamental pulsators with $\log P < 1.5$. Linear solutions: $\overline{M}_\lambda = a + b \log P$.

Z	a	b	σ
\overline{M}_B			
0.004	-0.90±0.03	-2.71±0.02	0.24
0.008	-0.93±0.03	-2.44±0.02	0.25
0.02	-1.21±0.02	-1.73±0.02	0.19
\overline{M}_V			
0.004	-1.32±0.02	-2.94±0.02	0.17
0.008	-1.37±0.02	-2.75±0.02	0.18
0.02	-1.62±0.01	-2.22±0.01	0.14
\overline{M}_R			
0.004	-1.61±0.02	-3.03±0.01	0.15
0.008	-1.65±0.02	-2.87±0.01	0.16
0.02	-1.88±0.01	-2.42±0.01	0.12
\overline{M}_I			
0.004	-1.92±0.01	-3.11±0.01	0.12
0.008	-1.95±0.01	-2.98±0.01	0.13
0.02	-2.14±0.01	-2.58±0.01	0.10
\overline{M}_J			
0.004	-2.28±0.01	-3.23±0.01	0.09
0.008	-2.29±0.01	-3.13±0.01	0.10
0.02	-2.41±0.01	-2.87±0.01	0.07
\overline{M}_K			
0.004	-2.61±0.01	-3.33±0.01	0.06
0.008	-2.61±0.01	-3.27±0.01	0.06
0.02	-2.67±0.01	-3.09±0.01	0.04

Table 4. Theoretical Period-Color relations.

Z	A	B	σ
$\overline{B - V} = A + B \log P$			
0.004	0.37 ± 0.01	0.30 ± 0.01	0.07
0.008	0.40 ± 0.01	0.37 ± 0.01	0.07
0.02	0.40 ± 0.01	0.51 ± 0.01	0.05
$\overline{V - R} = A + B \log P$			
0.004	0.26 ± 0.01	0.12 ± 0.01	0.03
0.008	0.26 ± 0.01	0.15 ± 0.01	0.03
0.02	0.24 ± 0.01	0.21 ± 0.01	0.02
$\overline{V - I} = A + B \log P$			
0.004	0.56 ± 0.01	0.22 ± 0.01	0.06
0.008	0.55 ± 0.01	0.28 ± 0.01	0.06
0.02	0.50 ± 0.01	0.38 ± 0.01	0.04
$\overline{V - J} = A + B \log P$			
0.004	0.90 ± 0.01	0.36 ± 0.01	0.09
0.008	0.87 ± 0.01	0.46 ± 0.01	0.10
0.02	0.75 ± 0.01	0.69 ± 0.01	0.08
$\overline{V - K} = A + B \log P$			
0.004	1.21 ± 0.01	0.50 ± 0.01	0.13
0.008	1.17 ± 0.01	0.62 ± 0.01	0.14
0.02	1.00 ± 0.01	0.93 ± 0.01	0.12

Table 5. Theoretical Color-Color relations.

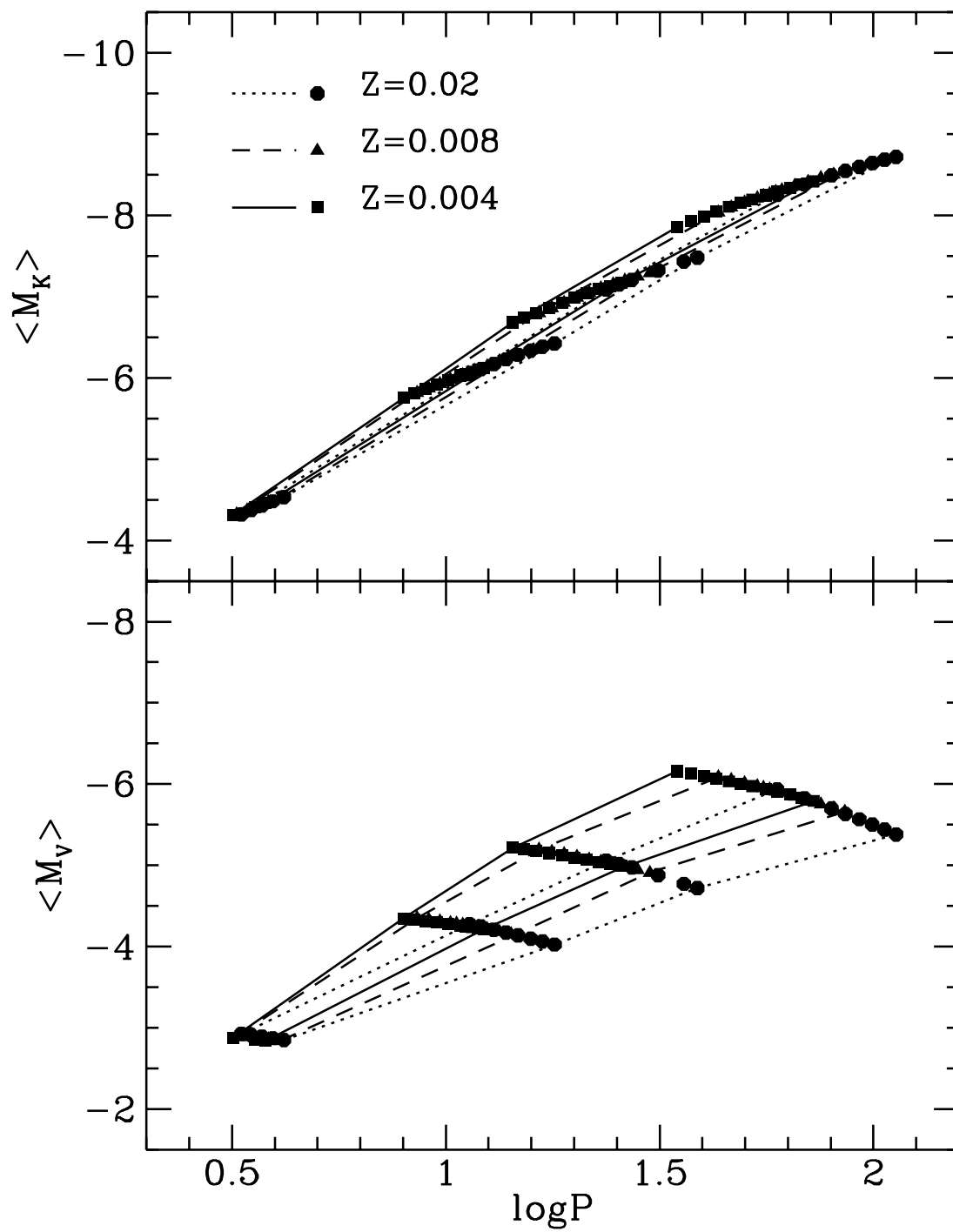
Z	C	D	σ
$\langle B \rangle - \langle V \rangle = C + D[\langle V \rangle - \langle R \rangle]$			
0.004	-0.25 ± 0.01	2.38 ± 0.03	0.01
0.008	-0.22 ± 0.01	2.39 ± 0.04	0.01
0.02	-0.16 ± 0.01	2.31 ± 0.02	0.01
$\langle B \rangle - \langle V \rangle = C + D[\langle V \rangle - \langle I \rangle]$			
0.004	-0.33 ± 0.01	1.28 ± 0.02	0.01
0.008	-0.30 ± 0.01	1.28 ± 0.03	0.01
0.02	-0.24 ± 0.01	1.28 ± 0.02	0.01
$\langle B \rangle - \langle V \rangle = C + D[\langle V \rangle - \langle J \rangle]$			
0.004	-0.29 ± 0.01	0.75 ± 0.02	0.01
0.008	-0.23 ± 0.02	0.74 ± 0.03	0.01
0.02	-0.13 ± 0.01	0.70 ± 0.01	0.01
$\langle B \rangle - \langle V \rangle = C + D[\langle V \rangle - \langle K \rangle]$			
0.004	-0.28 ± 0.01	0.54 ± 0.02	0.01
0.008	-0.24 ± 0.01	0.54 ± 0.02	0.01
0.02	-0.13 ± 0.01	0.52 ± 0.01	0.01

Table 6. Theoretical PLC relations.

Z	α	β	γ	σ
$\langle M_V \rangle = \alpha + \beta \log P + \gamma [\langle B \rangle - \langle V \rangle]$				
0.004	-2.54 ± 0.04	-3.52 ± 0.03	2.79 ± 0.07	0.04
0.008	-2.63 ± 0.04	-3.55 ± 0.03	2.83 ± 0.06	0.03
0.02	-2.98 ± 0.07	-3.72 ± 0.10	3.27 ± 0.18	0.07
$\langle M_V \rangle = \alpha + \beta \log P + \gamma [\langle V \rangle - \langle R \rangle]$				
0.004	-3.28 ± 0.03	-3.57 ± 0.02	6.93 ± 0.12	0.03
0.008	-3.31 ± 0.03	-3.59 ± 0.02	6.97 ± 0.11	0.03
0.02	-3.40 ± 0.04	-3.62 ± 0.05	7.09 ± 0.18	0.04
$\langle M_V \rangle = \alpha + \beta \log P + \gamma [\langle V \rangle - \langle I \rangle]$				
0.004	-3.55 ± 0.03	-3.58 ± 0.03	3.75 ± 0.07	0.03
0.008	-3.54 ± 0.03	-3.59 ± 0.02	3.74 ± 0.06	0.03
0.02	-3.61 ± 0.03	-3.59 ± 0.04	3.85 ± 0.09	0.03
$\langle M_V \rangle = \alpha + \beta \log P + \gamma [\langle V \rangle - \langle J \rangle]$				
0.004	-3.47 ± 0.03	-3.60 ± 0.03	2.26 ± 0.04	0.03
0.008	-3.40 ± 0.03	-3.60 ± 0.02	2.20 ± 0.04	0.03
0.02	-3.29 ± 0.04	-3.59 ± 0.04	2.11 ± 0.05	0.03
$\langle M_V \rangle = \alpha + \beta \log P + \gamma [\langle V \rangle - \langle K \rangle]$				
0.004	-3.44 ± 0.04	-3.61 ± 0.03	1.64 ± 0.03	0.04
0.008	-3.37 ± 0.04	-3.60 ± 0.03	1.61 ± 0.03	0.03
0.02	-3.25 ± 0.04	-3.55 ± 0.05	1.53 ± 0.04	0.04

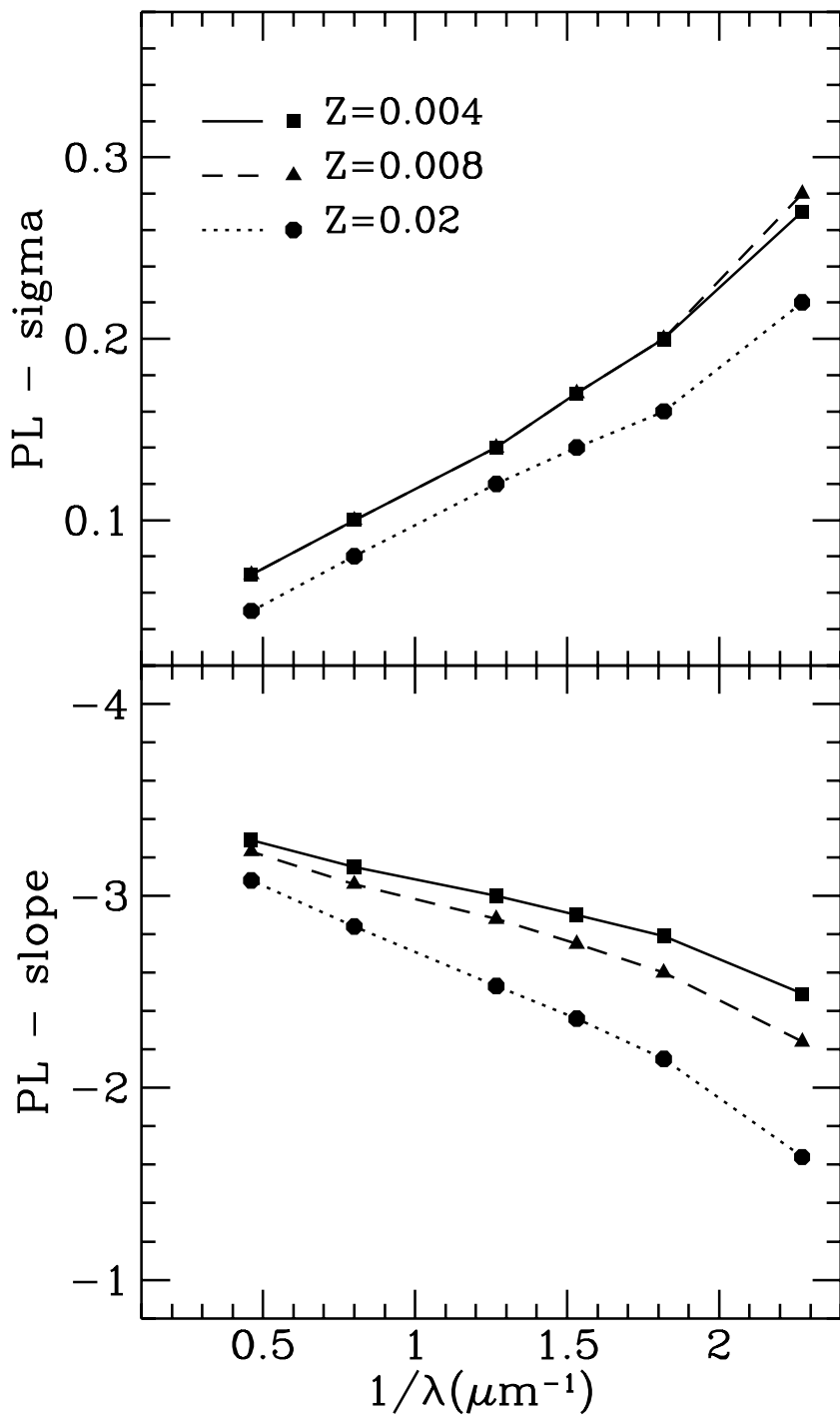
Table 7. Theoretical Wesenheit relations.

Z	a	b	σ
$W(B, V) = \langle M_V \rangle - 3.1 [\langle B \rangle - \langle V \rangle] = a + b \log P$			
0.004	-2.61 ± 0.05	-3.65 ± 0.02	0.05
0.008	-2.71 ± 0.04	-3.67 ± 0.02	0.04
0.02	-2.93 ± 0.07	-3.63 ± 0.03	0.07
$W(V, R) = \langle M_R \rangle - 5.29 [\langle V \rangle - \langle R \rangle] = a + b \log P$			
0.004	-3.15 ± 0.04	-3.46 ± 0.02	0.04
0.008	-3.17 ± 0.04	-3.46 ± 0.02	0.04
0.02	-3.24 ± 0.05	-3.43 ± 0.02	0.05
$W(V, I) = \langle M_I \rangle - 1.54 [\langle V \rangle - \langle I \rangle] = a + b \log P$			
0.004	-3.00 ± 0.10	-3.21 ± 0.05	0.10
0.008	-2.99 ± 0.10	-3.17 ± 0.04	0.10
0.02	-3.04 ± 0.10	-3.02 ± 0.04	0.10
$W(V, J) = \langle M_J \rangle - 0.39 [\langle V \rangle - \langle J \rangle] = a + b \log P$			
0.004	-2.86 ± 0.12	-3.15 ± 0.05	0.12
0.008	-2.83 ± 0.11	-3.12 ± 0.04	0.11
0.02	-2.83 ± 0.10	-3.02 ± 0.04	0.10
$W(V, K) = \langle M_K \rangle - 0.13 [\langle V \rangle - \langle K \rangle] = a + b \log P$			
0.004	-2.95 ± 0.10	-3.24 ± 0.05	0.10
0.008	-2.92 ± 0.09	-3.21 ± 0.04	0.09
0.02	-2.90 ± 0.08	-3.12 ± 0.03	0.08



This figure "pvn2.gif" is available in "gif" format from:

<http://arxiv.org/ps/astro-ph/9911441v1>



This figure "pvn4.gif" is available in "gif" format from:

<http://arxiv.org/ps/astro-ph/9911441v1>

